Electrochemical and spectroscopic investigations of the K2SO4-V2O5 molten electrolyte

Schmidt, Douglas S.; Winnick, Jack; Boghosian, Soghomon; Fehrmann, Rasmus

Published in:
Electrochemical Society. Journal

Link to article, DOI:
10.1149/1.1391721

Publication date:
1999

Document Version
Publisher's PDF, also known as Version of record

Journal of The Electrochemical Society, **146** (3) 1060-1068 (1999)
S0013-4651(98)01-004-0 CCC: $7.00

Electrochemical and Spectroscopic Investigations of the K_2SO_4–V_2O_5 Molten Electrolyte

Douglas S. Schmidt,[a,*,d] Jack Winnick,[a,*] Soghomon Boghosian,[b] and Rasmus Fehrmann[c,*]

[a]*School of Chemical Engineering, Georgia Institute of Technology, Atlanta, Georgia 30332-0100, USA*
[b]*Department of Chemical Engineering, University of Patras and Institute of Chemical Engineering and High Temperature Chemical Processes, GR-26500 Patras, Greece*
[c]*Department of Chemistry, Technical University of Denmark, DK-2800 Lyngby, Denmark*

A 60 mol % K_2SO_4/40 mol % V_2O_5 molten salt mixture was tested for electrochemical activity to determine its propensity for sulfate transport. Results of cyclic voltammetry showed a high electrochemical activity due likely to the reduction and oxidation of bulk, as opposed to minor, species. Most reductions and oxidations did not conform to diffusion-limited theory, and indicated the presence of stripping reactions. By Raman spectroscopy V(V) polymers were identified in the melt consisting predominantly of $VO_2(SO_4)_2^{3-}$ and VO_3^- units, while $VO_2SO_4^-$ units were also detected. By reduction of the eutectic mixture with SO_2 a V(IV) and a V(III) compound, most probably $K_4(VO)_3(SO_4)_5$ and $K_3V(SO_4)_3$, were isolated, as evidenced from infrared and electron spin resonance spectroscopy. These compounds might be involved in the electrochemically observed plating and stripping reactions.

Manuscript submitted January 2, 1998; revised manuscript received July 9, 1998.

The molten K_2SO_4/V_2O_5 system has recently attracted interest due to its possible use as an electrolyte in an electrolytic SO_x flue gas desulfurization process.[1-3] For this process to work, a low-melting point electrolyte is required. The eutectic composition 60 mol % K_2SO_4/40 mol % V_2O_5 has been reported to melt at 463°C,[1] 450°C,[4] or 430°C [5]; it is preferable to the ternary $(Li_{0.78}Na_{0.085}K_{0.135})_2SO_4$ eutectic which melts at 512°C.[6]

The main discrepancy between the two phase diagrams of the K_2SO_4-V_2O_5 system published so far[4,5] is the claimed existence of two different compounds, i.e., with the compositions $V_2O_5 \cdot K_2SO_4$ and $5V_2O_5 \cdot 3K_2SO_4$, respectively, based on powder X-ray data. No reports on the possible vanadium oxide or sulfate complexes formed in the melt are available. Nor has the redox chemistry or compound formation in this system during interaction with flue gas, or any gas, been reported. On the other hand, the $K_2S_2O_7$-V_2O_5 molten system has been explored extensively (Ref. 7 and references therein) because it is considered to be a realistic model melt of the industrial vanadium oxide-based SO_2 oxidation catalyst used for sulfuric acid production.[8,9] Here, vanadium (V) oxo sulfate complexes such as $VO_2SO_4^-$, $VO_2(SO_4)_2^{3-}$, $(VO)_2O(SO_4)_4^{4-}$ and their oligomers appear to be dominant among the melt species present.[7]

Recently[10] the X-ray structure of the compound $Cs_4(VO)_2O(SO_4)_4$ has been clarified, showing dimeric VO^{3+} units joined by an oxide bridge and achieving hexacoordination by the additional ligands of bidentate-coordinated sulfate groups. A similar structure was found[11] for the analogous K and Rb compounds. In melts in contact with SO_2-containing gases, V(V) is partly reduced to V(IV) complexes[12] such as $VO(SO_4)_2^{2-}$ and its oligomers, and to compounds of low solubility such as β-$VOSO_4$ and $K_4(VO)_3(SO_4)_5$. [13] In some cases even V(III) compounds are formed, e.g., $KV(SO_4)_2$ or $NaV(SO_4)_2$ and $Na_3V(SO_4)_3$ in the analogous $Na_2S_2O_7$-V_2O_5 system.[13] If the 60 mol % K_2SO_4/40 mol % V_2O_5 mixture is to be used as the electrolyte for sulfate transport, the characteristics of the molten sulfate/vanadium mixture need to first be determined.

Experimental

We analyzed this complex molten salt eutectic with two basic techniques: cyclic voltammetry was used first to determine the electrochemical activity of the melt; then Raman spectroscopy was employed in an attempt to identify the active species.

Cyclic voltammetry.—Cyclic voltammetry utilized 4 N (Alfa Products) gold flag electrodes created by cutting foil to size, and welding to an Au wire lead (0.127 mm diam, 99.99% purity, Johnson Mathey). A glass sheath sealed the Au reference and counter electrode leads and created a fixed area for the electrochemical study. The electrode could be immersed to a known depth in the molten salt. The working electrode size was 0.38 cm^2.

A pseudo-reference nonthermodynamic reference electrode was used in these experiments. The pseudo-reference provided reproducible results with low ohmic loss at small potential differences. An Au wire in the pseudo-reference electrode encased in an alumina sheath was continually bathed in an isolated flow of 3000 ppm SO_2, 3% O_2, N_2 (Matheson gas mixtures), while the gold maintained contact with the molten salt through the open bottom.

The electrodes and melt were encased in a glass container that protruded from a high-temperature furnace (in-house manufacture) which was maintained at 480°C. This allowed positive atmospheric control as seals could be made at lower temperature.

The potential was controlled by an EG&G PAR model 273 scanning potentiostat/galvanostat with digital iR compensation and a 4 V scanning range. Output was monitored by a Hewlett Packard 7015B X-Y recorder with 200 V maximum floating peak input, optional time and voltage scales, a 50 cm/s slew speed with an overshoot of <2% of full scale, and a very low signal/noise ratio. Scans began at the rest potential with respect to the pseudo-reference, and the potential was allowed to return to that rest potential between scans.

The 60 mol %/40 mol % K_2SO_4/V_2O_5 mixture (450 g total) was prepared by mixing K_2SO_4 (Fisher, dried for 24 h at 250°C in air and kept in a dessicator until used) with V_2O_5 (Sigma, used as received) in the proper weight percentages. This mixture was milled with alumina media for 24 h prior to use.

Gas compositions were controlled by using premixed $SO_2/O_2/N_2$ (Matheson) or by mixing 99.9% O_2 (Air Products) and 99.99% N_2 (Air Products) as needed with Matheson flowmeters. Three gas compositions were used: 100% N_2, 50% O_2/50% N_2, and 3000 ppm SO_2/3% O_2/N_2. Scans were performed with gas flowing over the surface of the melt. Upon changes of atmosphere, gas was allowed to bubble through the melt overnight.

High-temperature Raman spectroscopy.—Sample preparation.—The samples were prepared by mixing V_2O_5 (Cerac, Pure 99.9%) and K_2SO_4 (Fluka) which was dried by heating in vacuo at 300°C for 4 h. All handling of chemicals and filling of the Raman optical cells (made of cylindrical fused silica tubing (6 ± 0.1 mm o.d., 2 ± 0.1 mm i.d., and ~4 cm long for the part containing the molten salts)) took place in a nitrogen-filled glove box. The samples were sealed under a low pressure (ca. 0.2 atm) of O_2 (L'Air Liquide, 99.99%) in order to stabilize vanadium in the pentavalent state and were equilibrated at 540°C for up to 7 days before recording the

* Electrochemical Society Active Member.
[a] Present address: Siemens-Westinghouse, Pittsburgh, PA 15235.

S0013-4651(98)01-004-0 CCC: $7.00

Raman spectra. Dark red-brown melts were obtained in this way. Sealing the samples under oxygen proved to be critically important for avoiding partial self-reduction of V(V) to V(IV) whereby a gradual color change to dark green and precipitation of crystalline solids would take place.

Raman spectra.—Raman spectra were obtained by exciting with the 647.1 nm line of a Spectra Physics Stabilite model 2017 krypton-ion laser and the 488.0 nm line of a Spectra Physics model 164 argon-ion laser. The scattered light was collected at an angle of 90° (horizontal scattering plane), rotated with a 90° image rotator, and analyzed with a Spex 1403 0.85 m double monochromator possessing a vertical entrance slit and equipped with a −20°C cooled RCA photomultiplier and EG&G/ORTEC rate meter and photon-counting electronics. The optical furnace (suited for recording Raman spectra at temperatures up to 950°C) used and the procedures followed for obtaining Raman spectra at high temperatures have been described in detail elsewhere.[14] It should be pointed out here that recording of the Raman spectra at elevated temperatures from these very dark-colored, viscous, and hygroscopic melts was very difficult due to strong absorption of the incident exciting laser light. In certain cases, in order to enable the succesful recording of Raman spectra, light reflected and/or dispersed from the walls of the quartz sample containers had to be masked by proper adjustment of the monochromator entrance slit height.

IR and ESR spectroscopy.—The infrared spectra were recorded for samples in KBr on a Perkin Elmer 1710 Fourier transform infrared (FTIR) spectrometer. Electron spin resonance (ESR) spectra were recorded on grounded samples at room temperature in the X-band on a Bruker EMX EPR spectrometer.

Results

Cyclic voltammetry.—A typical stabilized scan in the $SO_2/O_2/N_2$ environment can be seen in Fig. 1. The first positive scan from rest resulted in peaks I_1 and II_1. Peak I_c was observed duirng the next negative scan. After reversing at the negative switching potential, two additional peaks, II_c and III_c, were observed, followed by a large oxidation peak I_a and smaller oxidation peak II_a. Peaks I_1 and II_1 were not observed when the first scan was negative from the rest potential, although all other peaks were observed. Scans were generally found to be stable after the first positive scan when initially scanning positive; or, when initially scanning negative, with the first scan.

An unusual reduction is indicated by the presence of peaks II_c and III_c only on the return scan. Peak I_a appears to be a stripping peak due to its characteristic shape and size. Peak currents (i_p) are substantial, exceeding 1 A/cm^2 in many cases, indicative of reduction and oxidation of readily available species at high concentration.

The dependence of these peaks on one another became apparent when the negative switching potential was allowed to increase while holding the positive switching potential at +2.000 V (vs. pseudo-reference; chosen as a switching potential well positive of observed peaks) and scanning at 500 mV/s. Figure 2 shows stabilized scans for the process, in which the first scan is positive and shows peaks I_1 and II_1, and subsequent stable scans. A substantial effect of switching potential and peak dependence can be observed visually with these new scans. This dependence was seen for all atmospheres and is shown here for the $SO_2/O_2/N_2$ environment. Figure 3 shows the peak potentials (E_p) and current densities with changes in negative switching potential; Fig. 4 shows peak potentials and peak current densities vs. the square root of the scan rate. Peak potentials for I_1 and II_1 did not vary with the square root of the scan rate. These results are again for the $SO_2/O_2/N_2$ environment.

Most of the peak currents do not conform to theoretical diffusive limitations (absolute peak current density varying linearly with the square root of scan rate and a positive slope). Incomplete iR compensation likely contributed to the observed effect, and slow kinetics may also be possible. Finally, the negative switching potential had a strong effect on the peak current density and potential, with i_p and E_p increasing with decreases in the negative switching potential for most peaks.

Three peaks did approach diffusion-limited theory: I_1, II_1, and I_c. The dependence of i_p on the square root of the scan rate in different atmospheres is shown in Fig. 5, 6, and 7. Of these, the constant

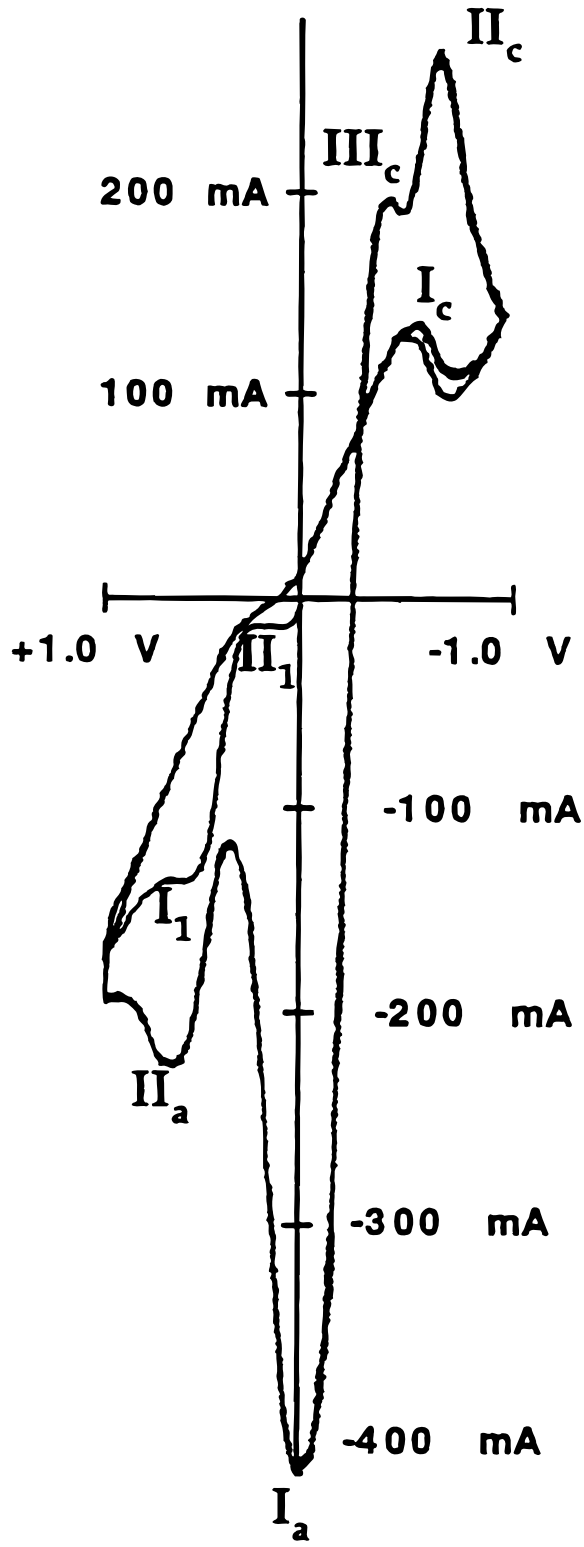

Figure 1. Typical cyclic voltammogram of a 500 mV/s scan of K_2SO_4/V_2O_5 melt at 480°C under 3000 ppm SO_2/3% O_2/N_2 atmosphere on gold electrodes. Reduction current is positive and negative potential is to the right.

S0013-4651(98)01-004-0 CCC: $7.00

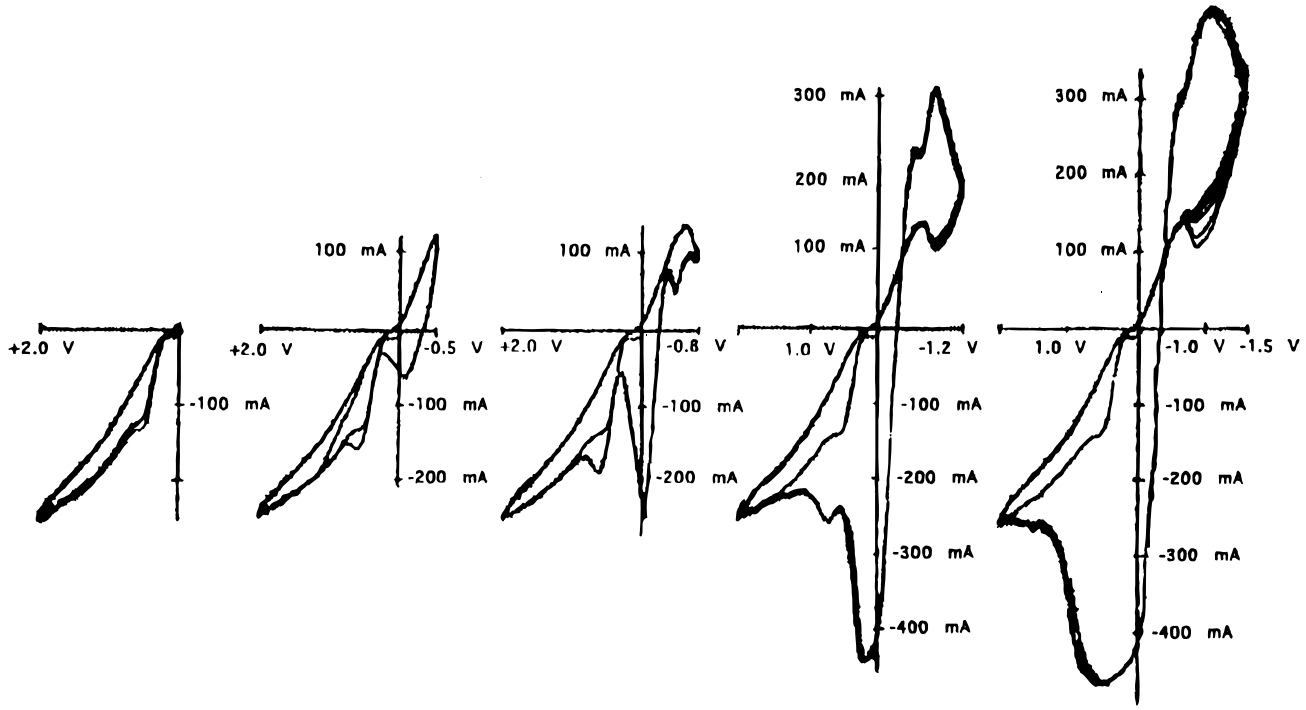

Figure 2. Effect of changes of negative switching potential on cyclic voltammograms at 500 mV/s.

potentials of peaks II_1 and I_c with scan rate suggested a reversible mechanism, whereas the variance of I_1 potentials with scan rate suggested an irreversible mechanism. The $E_{p/2}$ values of peak I_c were used to determine approximate values of n using

$$n = \frac{2.2RT}{(E_p - E_{p/2})F} \quad [1]$$

To evaluate αn for peak I_1

$$\alpha n_a = \frac{1.857RT}{(E_p - E_{p/2})F} \quad [2]$$

was used. Peak II_1 could not be satisfactorily evaluated due to the error associated with $E_{p/2}$ measurement of the recorded voltammograms. The results are shown in Table I. Uncompensated iR may introduce a positive error in n of about 3 to 4 mV. Uncompensated impedance arising from thin films at the electrode surface, however, could lower the apparent value of n. For these reasons, the actual number for n was deduced to be 1 equiv/mol, and n_a 2 equiv/mol with an α of 0.5.

For peaks II_1 and I_c it is possible to infer the term $C_i D_i^{1/2}$ for each curve using the $n = 1$ equiv/mol determined for peak I_c and assuming a value of $n = 1$ equiv/mol for peak II_1 applying

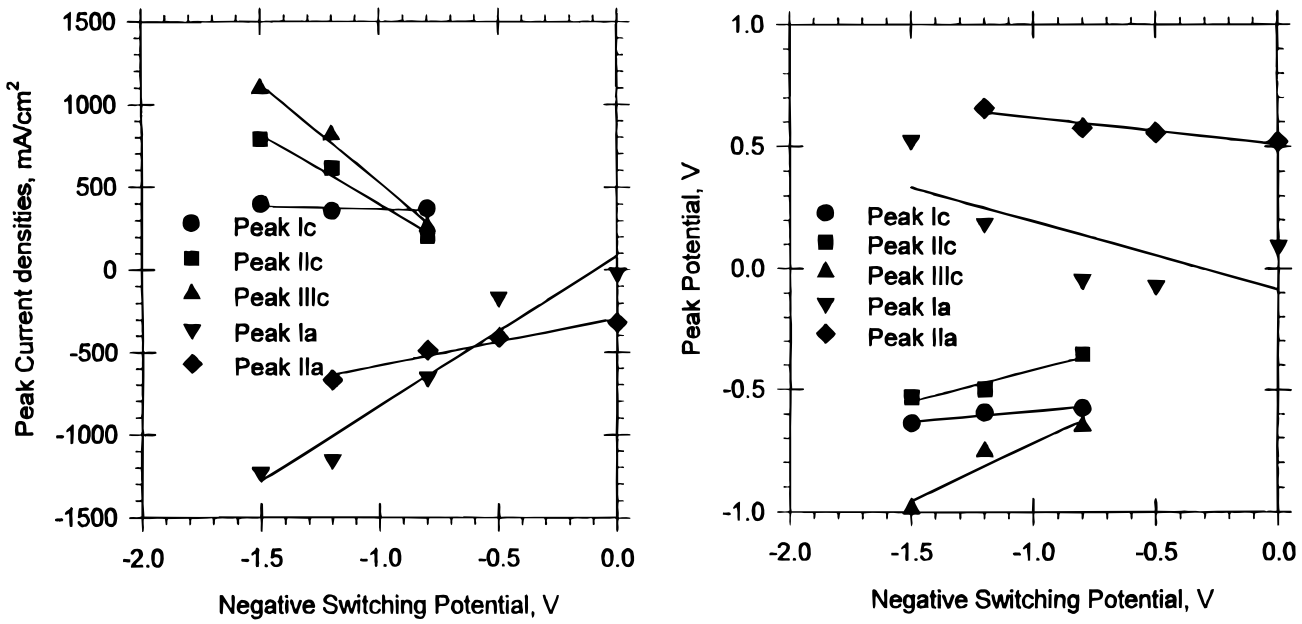

Figure 3. Peak currents and potentials at varying negative switching potential. Lines denote best linear fit.

S0013-4651(98)01-004-0 CCC: $7.00 © The Electrochemical Society, Inc.

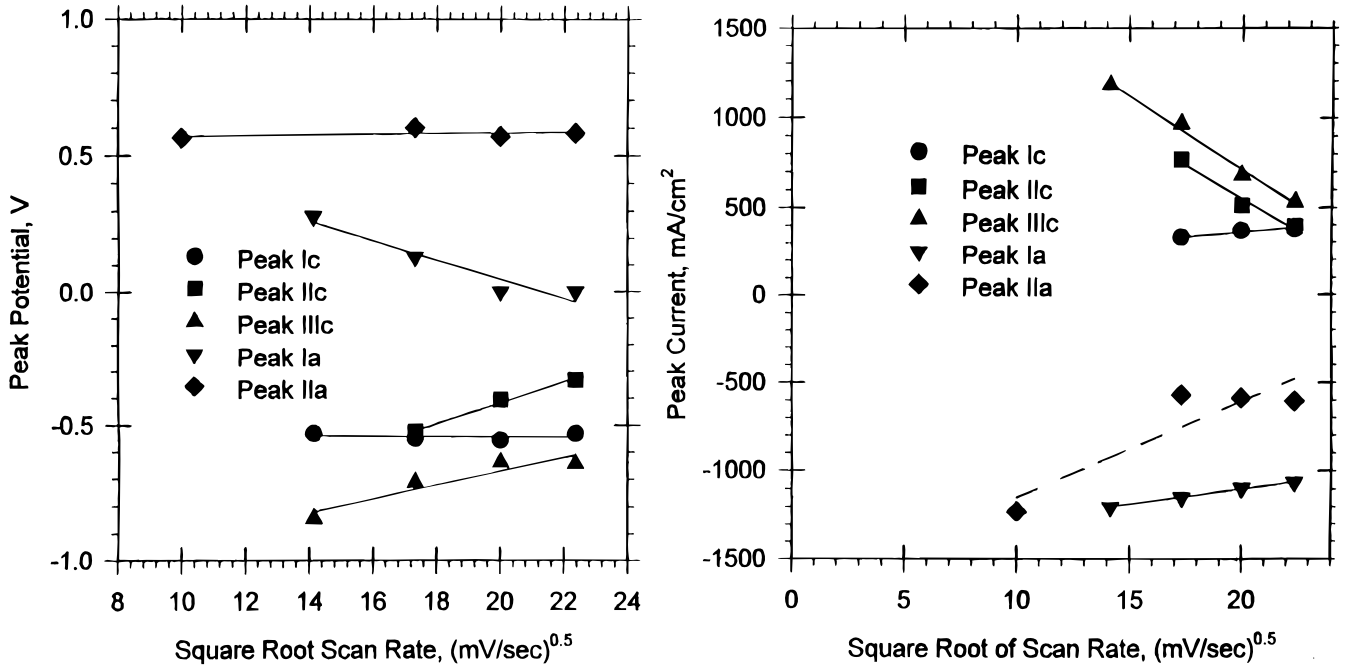

Figure 4. Peak currents and potentials at varying scan rate. Solid lines denote best linear fit. Dashed line indicates uncertain linearity.

$$i_p = 0.4463nFC_i\left(\frac{nF}{RT}\right)^{1/2}\nu^{1/2}D_i^{1/2} \quad [3]$$

For peak I_1, the n and αn_a derived earlier were used with

$$i_p = 0.4nFC_i\left(\frac{\alpha n_a F}{RT}\right)^{1/2}\nu^{1/2}D_i^{1/2} \quad [4]$$

to determine $C_iD_i^{1/2}$. These values are listed in Table II.

The small effect of the O_2/N_2 and the larger effect of $SO_2/O_2/N_2$ in comparison to the N_2 environment was expected. Boreskov[15] showed that O_2 has a penetration depth of 100-200 Å in sulfate-vanadia melts, whereas SO_2 has a very high apparent solubility, due to possible reactions with the melt. With the electrodes immersed 3 cm, these melt properties became apparent. This also indicates a stronger mechanism dependence on SO_2 than O_2, i.e., an indirect chemical oxidation by oxygen.

To provide further insight into the initial conditions of the melt, the $C_iD_i^{1/2}$ ratios were calculated for peaks I_1 and II_1 in comparison to peak I_c (see Table III). Assuming peak I_1 represents V(IV) in chemical equilibrium in the melt, it is possible to compare observed concentration ratios with theoretical values. Based on the equation

$$V_2O_5 \rightleftarrows V_2O_4 + \frac{1}{2}O_2 \quad \Delta G_f^o\ (750\ \text{K}) = 96.45\ \text{kJ/mol} \quad [5]$$

at 477°C and $P_{O_2} = 0.03$ atm, data for ΔG_f^o from the thermochemical tables of JANAF[16] predict a ratio of C_{V5+}/C_{V4+} of 9.0×10^5. While far different from any ratio determined, both show V(V) to be very much the dominant vanadia oxidation state. The difference suggests that composition and interactions in the melt are not ideal.

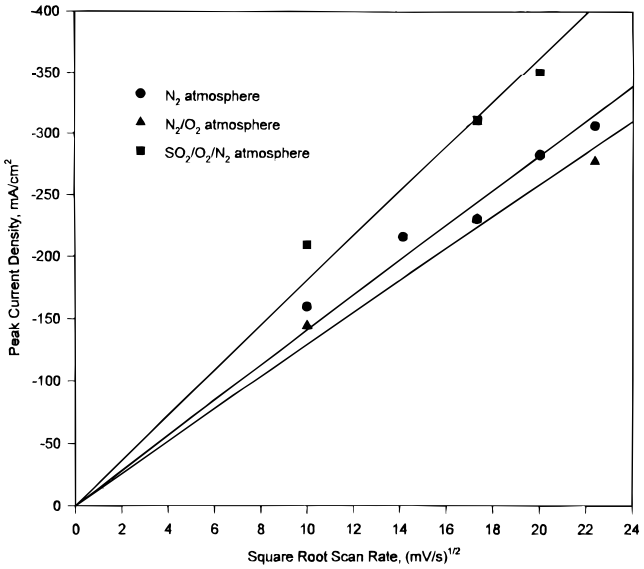

Figure 5. Peak I_1 current density with scan rate under different atmospheres. Lines denote best fit with forced origin intercept.

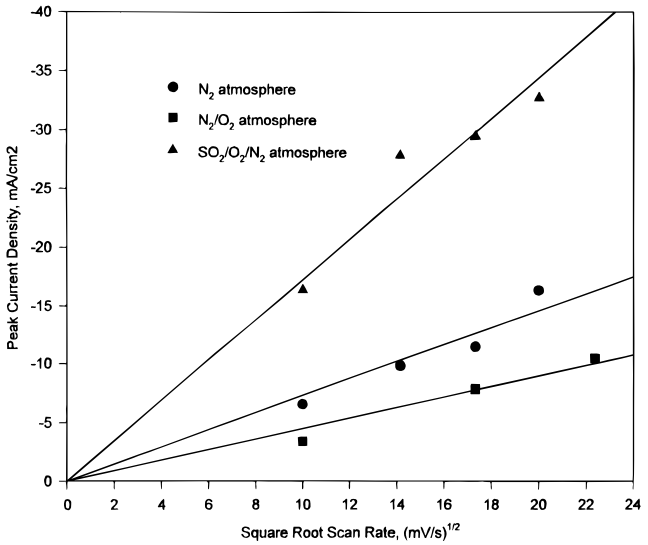

Figure 6. Peak II_1 current densities with scan rate under different atmospheres. Lines denote best fit with forced origin intercept.

S0013-4651(98)01-004-0 CCC: $7.00

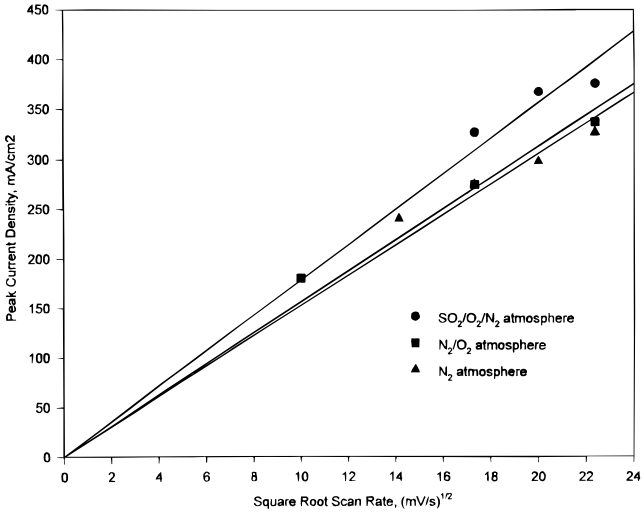

Figure 7. Peak I_c current densities with scan rate under different atmospheres. Lines denote best fit with forced origin intercept.

Because a reversible peak was observed immediately upon moving negative from the rest potential with respect to our pseudo-reference, and a smaller diffusion-limited peak was observed immediately when the potential became positive of the rest potential, it was assumed that the pseudo-reference was resting at the V(V)/V(IV) couple. The additional observations discussed below lend evidence to this assumption.

Raman spectroscopy.—Several binary K_2SO_4-V_2O_5 mixtures were placed in cells sealed under 0.2 atm of oxygen and Raman spectra of the melts obtained after equilibration were recorded in the temperature range 450-570°C. The data obtained did not indicate any temperature dependence for the relative Raman intensities. The only temperature-dependent feature appears to be the increase of the signal-to-noise ratio in the lower-temperature region. Therefore, data are presented for representative samples at 490°C which was the lowest temperature at which all samples studied were in the liquid state. Finally, it should be pointed out that the 647.1 nm excitation used overlaps with the tail of the electronic charge-transfer transition of V(V) and therefore the spectra obtained are very likely to be of preresonance character leading to enhancement of the band intensities due to the V(V) species present.

Table I. Values for n and αn_a for peaks I_c and I_1, under different atmospheres.

Atmosphere	Peak I_c, n, equiv/mol	Peak I_1, αn_a, equiv/mol
$SO_2/O_2/N_2$	0.46 ± 0.05	0.87 ± 0.28
O_2/N_2	0.38 ± 0.11	0.84 ± 0.31
N_2	0.62 ± 0.33	0.78 ± 0.19

Table II. Values of $C_iD_i^{1/2}$ for peaks I_c, I_1, and II_1, under different atmospheres.

	Atmosphere	$C_iD_i^{1/2} \times 10^7$, mol/cm^3 (cm^2/s)$^{1/2}$
Peak I_c		
	SO_2/O_2N_2	4.17
	O_2/N_2	3.68
	N_2	3.57
Peak I_1		
	$SO_2/O_2/N_2$	3.80
	O_2/N_2	2.73
	N_2	2.95
Peak II_1		
	$SO_2/O_2/N_2$	0.39
	O_2/N_2	0.11
	N_2	0.18

Table III. Comparison of $C_iD_i^{1/2}$ ratios for peaks I_c, I_1, II_1. A ratio of peak concentration.

Peak current (i_p) ratio/atmosphere	N_2	O_2/N_2	$SO_2/O_2/N_2$
(Peak I_c)/(Peak I_1)	1.10	1.35	1.21
(Peak I_c)/(Peak II_1)	10.72	33.45	19.8

Figure 8 shows Raman spectra obtained for the molten K_2SO_4-V_2O_5 mixtures with compositions $X(V_2O_5) = 0.33, 0.40, 0.45$, and 0.50 (spectra b-e). Spectra obtained for the molten reference systems $V_2O_5 \cdot K_2S_2O_7 \cdot 2\,K_2SO_4$ (a) and $NaVO_3$ (f) are also included in Fig. 8 for comparison. The Raman spectrum of the $V_2O_5 \cdot K_2S_2O_7 \cdot 2K_2SO_4$ mixture has previously been assigned[17,18] to the molten complex species $VO_2(SO_4)_2^{3-}$ (presumably occurring as an oligomer of polymer) formed by the reaction

$$V_2O_5 + S_2O_7^{2-} + 2SO_4^{2-} \rightarrow 2VO_2(SO_4)_2^{3-} \qquad [6]$$

The Raman spectra of fused alkali metavanadates have not been published before. The spectra obtained for molten $NaVO_3$ are in fair

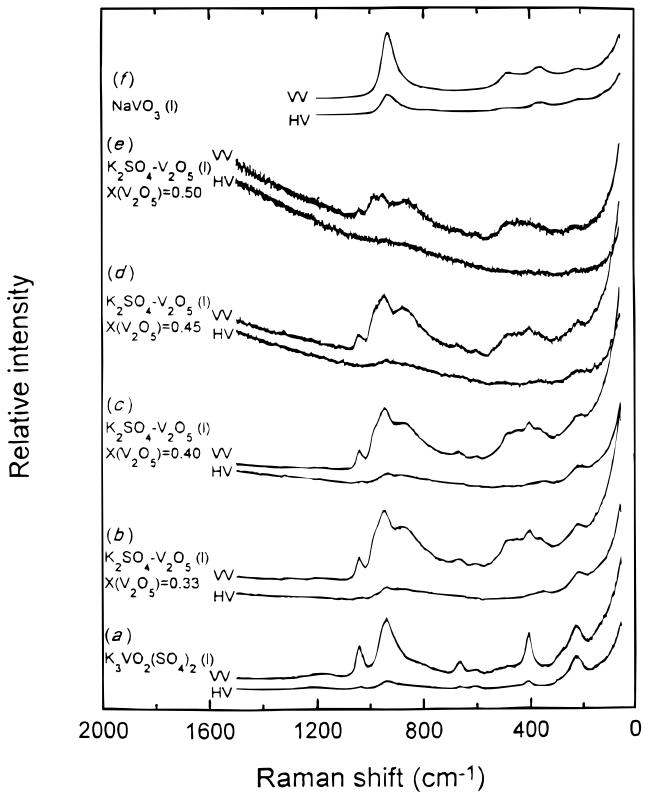

Figure 8. Raman spectra of molten $K_2S_2O_7 \cdot V_2O_5 \cdot 2K_2SO_4$ at 450°C (a); molten K_2SO_4-V_2O_5 mixtures at 490°C with X (V_2O_5) = 0.33 (b), 0.40 (c), 0.45 (d), and 0.50 (e) and molten $NaVO_3$ at 645°C (f). VV and HV denote vertical-vertical and horizontal-vertical spectra polarization, respectively. λ_o = 647.1 nm for (a-e) and 488.0 nm for (f); laser power, w = 175 mW for (a-e) and 70 mW for (f); scan speed, ss = 48 cm^{-1} min^{-1} for (a), 30 cm^{-1} min^{-1} for (b), 24 cm^{-1} min^{-1} for (c, d), 18 cm^{-1} min^{-1} for (e), and 60 cm^{-1} min^{-1} for (f); time constant, τ, l s for (a), 3 s for (b-e), and l s for (f); spectral slit width, sww = 6 cm^{-1} min^{-1}.

S0013-4651(98)01-004-0 CCC: $7.00

agreement with previously reported spectra of "quenched" $NaVO_3$ melts.[19] The $NaVO_3$ crystal structure reveals that the compound consists of infinite chains of tetrahedral VO_4 units sharing corners and the same structural model can be adopted for molten $NaVO_3$. Attempts to obtain Raman spectra for molten KVO_3 failed due to complete absorption of the laser line by the very dark melt. The spectra obtained for molten $NaVO_3$-Na_2SO_4 mixtures showed no bands due to sulfate groups, indicating that no complex formation occurs between VO_3^- and SO_4^{2-}. The bands due to free uncoordinated SO_4^{2-} are probably obscured by the VO_3^- bands of which the intensities might in turn have been strongly enhanced due to the resonance conditions described above. Excitation of the K_2SO_4-V_2O_5 melts with compositions $X(V_2O_5) = 0.33$ and 0.40 (spectra b and c) gives rise to characteristic bands at 1043, 982, 950, 875, 670, 605, 489, 450, 362, and 220 cm^{-1}, which are all polarized except for the 220 cm^{-1} band which is depolarized. This can be interpreted as indicating a low symmetry for the complex(es) formed, but it could also be a result of the preresonance character of the spectra. The spectra appear to consist mainly of superposition of bands due to $VO_2(SO_4)_2^{3-}$ and VO_3^- [spectra (a) and (f), respectively] plus the 982 cm^{-1} shoulder band and the strong broad band at 875 cm^{-1}, which however is present but much weaker in spectrum (a) of $VO_2(SO_4)_2^{3-}$. Formation of the $VO_2(SO_4)_2^{3-}$ and VO_3^- units can be accounted for by the reaction

$$V_2O_5 + 2SO_4^{2-} \rightarrow VO_2(SO_4)_2^{3-} + VO_3^- \quad [7]$$

An increase in the V_2O_5 mole fraction results in (*i*) enhancement of the 982 cm^{-1} shoulder band intensity which is completely resolved in spectrum (e) of the 1:1 K_2SO_4-V_2O_5 molten mixture and (*ii*) extreme lowering of the signal-to-noise ratio due to very strong absorption of the excitation line from the dark melt which made the recording of the Raman spectra very dificult. The 1043 cm^{-1} band is assigned[17] to the terminal stretching of the short V=O involving hexacoordinated vanadium of the $VO_2(SO_4)_2^{3-}$ complex unit. The 982 cm^{-1} band is assigned to terminal V=O stretching involving tetracoordinated vanadium of the $VO_2SO_4^-$ unit which appears to be formed in significant amounts in samples with increasing V_2O_5 contents, where it is stoichiometrically favored over the $VO_2(SO_4)_2^{3-}$ and formed according to the scheme

$$V_2O_5 + SO_4^{2-} \rightarrow VO_2SO_4^- + VO_3^- \quad [8]$$

The 950 cm^{-1} band contains contributions from terminal S-O stretchings of SO_4^{2-} groups and terminal V-O stretchings of the VO_3^- groups where vanadium is also tetracoordinated. The 875 cm^{-1} band is assigned to bridging S-O stretchings involving oxygen coordinated to vanadium. Detailed assignment of the remaining bands is beyond the scope of the present article.

IR and ESR spectroscopy.—Compounds formed by reduction of the eutectic melt in SO_2 atmosphere have been isolated and characterized. The chemicals of the 60 mol %/40 mol % K_2SO_4/V_2O_5 eutectic mixture were weighed in a glass ampule and sealed under 0.9 atm SO_2. The molar ratio of SO_2 to V_2O_5 was four, making a complete reduction to V(III) possible. The ampule was heated to 600°C in a ceramic tubular furnace for 1 h and then slowly cooled to 100°C during 50 h by a linear temperature program before it was removed from the furnace. The ampule was inspected in a microscope, and small, light-green, bluish green, and black crystals were observed. The light-green crystals could be isolated after opening the ampule whereas the bluish green crystals could not be separated from the black matrix of the solidified eutectic melt. The light-green crystals were too small for single-crystal X-ray investigations, but chemical analysis and IR spectroscopy could be carried out.

The IR spectrum of the compound is displayed in Fig. 9. The spectrum exhibits typical features of coordinated sulfate groups with ν_1 at 980 cm^{-1} and ν_3 split into three components at 1010, 1140, and 1225 cm^{-1}. The ν_2 and ν_4 bending modes are found below 700 cm^{-1} as expected. The spectrum is very similar to what has earlier[20] been recorded for the V(III) compound $Na_3V(SO_4)_3$. Furthermore chemical analysis [atomic absorption spectroscopy (AAS)] of the green crystal showed a molar ratio K/V = 2.92 in close agreement with the expected formula $K_3V(SO_4)_3$, for the potassium analogue of $Na_3V(SO_4)_3$.

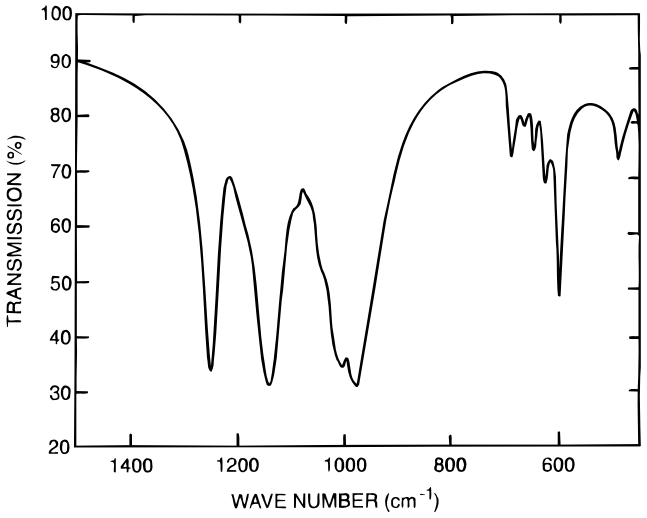

Figure 9. Infrared spectrum of the isolated V(III) compound in KBr.

The ESR spectrum of the bluish green-black matrix mixture is shown in Fig. 10. The spectrum is almost isotropic with g_o = 1,968(1) and ΔH_{pp} = 99(2)G. Because V(V) of the matrix and V(III) of the green compound are ESR silent, these possible contaminates will not interfere with the spectrum of a V(IV) compound. Indeed, the observed spectrum is identical with the spectrum[13] for the V(IV) compound, $K_4(VO)_3(SO_4)_5$ isolated earlier[21] from $K_2S_2O_7$-V_2O_5 melts reduced by SO_2.

Discussion

Consider the initial constituents, V_2O_5 and K_2SO_4, and the original molar ratio V/K of charging: 0.80/0.60 or 1.33 (two vanadium ions per 1 mole V_2O_5). The ratio of peak I_c to that of I_1 averages 1.22. In the $SO_2/O_2/N_2$ atmosphere, this ratio differed by only 8.3%. If the major component of change is the oxidation state and availability of V(V), and this was the ratio of initially available vanadium to sulfate, this trend would be expected, modified by complex-melt interaction.

The ratio of peak I_c to II_1 decreased significantly as the atmosphere became more reducing. Peak I_c relative to that of peak II_1 also

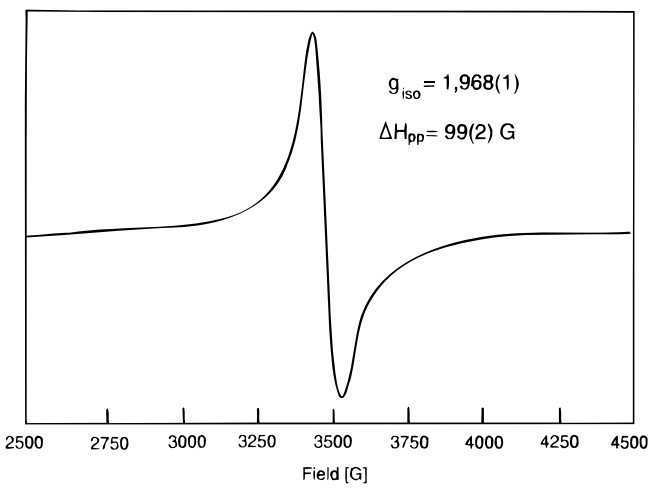

Figure 10. ESR spectrum of the isolated V(IV) compound. The isotropic *g* value and the linewidth (ΔH_{pp}) are as indicated.

S0013-4651(98)01-004-0 CCC: $7.00

decreased, but at what was apparently a much faster rate. If it is assumed, as before, that I_c represented initially available V(V), it would be expected that the more reducing the atmosphere, the less V(V) would be available due to greater reduction to lower vanadium oxidation states. An increase in peak II_1 combined with a decrease in peak I_c would best explain this significant change in ratios. If peak II_1 represented initially available V(IV), the observed trend would comply with expectations.

Equilibrium of vanadium according to

$$V(V) \underset{SO_3}{\overset{SO_2}{\rightleftharpoons}} V(IV) \underset{SO_3}{\overset{SO_2}{\rightleftharpoons}} V(III) \qquad [9]$$

is important using vanadium-based systems.[13] It is generally accepted that vanadium cannot be reduced to V(2+) or the metal vanadium in melts containing chlorides, metaphosphates, or sulfates.[22]

The results of the Raman spectroscopic study show that at least three different V(V) species coexist in the 60/40 mol % K_2SO_4-V_2O_5 melt. It appears that the predominant complex units formed are the VO_3^- and $VO_2(SO_4)_2^{3-}$ and that the $VO_2SO_4^-$ unit is also formed to a lesser extent. Increasing amounts of $VO_2SO_4^-$ are found for $X(V_2O_5) > 0.40$. Reactions 7 and 8 account for the formation of the above complex units. The VO_3^- species is most probably polymeric in the molten state as in the crystalline state forming infinite chains of tetrahedral VO_4 units sharing corners, Eq. 10

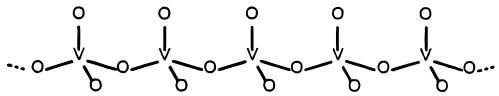
$(VO_3)_n^{n-}$ [10]

Adding sulfate to the vanadate melt does not appear to affect the VO_3^- chains but dissolves as uncoordinated SO_4^{2-}. This is supported by phase studies of the binary KVO_3-K_2SO_4 system[23] which show that no compound is formed. The $VO_2(SO_4)_2^{3-}$ complex occurs most probably also in the form of polymeric chains[17,18,24] in which the complex units are linked by bidentate bridging sulfate groups and the six-coordinated vanadium is found in the usual distorted octahedral environment illustrated by

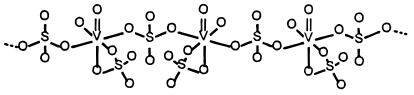
$(VO_2(SO_4)_2)_n^{3n-}$ [11]

Finally, the $VO_2SO_4^-$ species may similarly form polymeric chains in which the $VO_2SO_4^-$ units are linked by bidentate bridging sulfate groups and possess four-coordinated V(V) in a distorted tetrahedral environment as indicated by recent nuclear magnetic resonance (NMR) studies on molten $CsVO_2SO_4$. [25,26] A simple structural model describing this configuration is depicted by

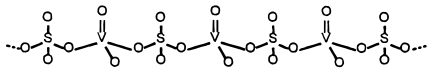
$(VO_2(SO_4))_n^{n-}$ [12]

It is evident that mixed copolymeric chains may be also formed consisting of the three complex units. It should be pointed out that the relative positions of the V=O stretching modes for the three complex units $VO_2(SO_4)_2^{3-}$, $VO_2SO_4^-$, and VO_3^- at 1043, 982, and 950 cm^{-1} is in conformity with the respective coordination numbers for the vanadium atom 6, 4, and 4 discussed above. It is known[27] as a general hard-and-fast rule that the V=O bond length is significantly shorter in VO_6 rather than in VO_4 environments whereby a higher V=O stretching frequency is expected for the former in the Raman spectrum. Furthermore the values of 982 and 950 cm^{-1} for the tetracoordinated V(V) species indicate a shorter V=O bond for $[VO_2SO_4]_n^{n-}$ and a more uniform environment around vanadium in $(VO_3)_n^{n-}$.

Reduction of the possible V(V) entities to V(IV) may take place by the following electrode processes

$$VO_3^- + SO_4^{2-} + e^- \rightleftarrows VOSO_4 + 2\,O^{2-} \qquad [13]$$

$$VO_2SO_4^- + e^- \rightleftarrows VOSO_4 + O^{2-} \qquad [14]$$

$$VO_2(SO_4)_2^{3-} + e^- \rightleftarrows VO(SO_4)_2^{2-} + O^{2-} \qquad [15]$$

These three reductions of V(V) may all occur at nearly the same potential, i.e., corresponding to peak I_c at -0.7 V, overlapping each other on the scan; or alternatively, one of the reactions, probably Eq. 13, may be so dominant that the others are hidden.

Work by Franke and Winnick[28] and Bazarova et al.[29] proposed the following reduction of vanadium

$$[K_2O{\cdot}V_2O_5{\cdot}4SO_3] + 2e^- \rightleftarrows [K_2O{\cdot}V_2O_4{\cdot}3SO_3] + SO_4^{2-} \qquad [16]$$

occurring at approximately $E_p = +0.7$ V vs. Ag/Ag^+ in pyrosulfate melts. The number of electrons involved in the V(V) reduction varied from one to two depending on the gas composition.[28] Other electrochemical studies of Durand[30] and Bjerrum[31] in pyrosulfate melts showed the reduction to be a one-electron reaction as in the present study in sulfates. However, the polymeric vanadium (V) complexes present in the 60% K_2SO_4-40% V_2O_5 melt investigated here differ from the predominantly dimeric V(V) species found[17] in the pyrosulfate melts up to 33% V_2O_5. Therefore, the redox processes taking place in the different media may be fundamentally different. Voltammetric investigations of Dojcinovic[32] above 500°C in 80% Li_2SO_4-20% K_2SO_4 melts at low concentrations of V(V), showed that V(V), V(IV), and probably also V(III) species were formed in the melt, as in the present study. The number of electrons involved in the redox reactions was not stated. Wolfe and Caton[33] recorded $E_o = +0.394$ V vs. Ag/Ag^+ at 700°C, very close to that of Franke, in a phosphate melt for a one-electron reduction of V(V)/V(IV). Laitinen and Rhodes[34] showed vanadium reduction to a mixed state in a LiCl/KCl melt as

$$6V_2O_5 + 2Li^+ + 4e^- \rightleftarrows Li_2O + 2V_2O_4 + 4V_2O_5 + O^{2-} \qquad [17]$$

with the reduction of V(V) to V(IV) at -0.6 V vs. Pt/Pt^{2+} reference. With the one-electron process, peak I_c is very likely the reduction of vanadium.

Peak II_c represents additional reduction of V(V). As scanning slowed, peak II_c and III_c current increased, while peak Ic showed a relatively linear fit with $\nu^{1/2}$. Peaks II_c and III_c were not dependent on diffusion; they were effectively nonexistent initially. They did depend on the fact that V(V) was first reduced at peak I_c. As the switching potential neared the peak potential for peak I_c, peaks Ic and II_c overlapped, suggesting that they are identical reactions.

Because the $VOSO_4$ formed initially, by reduction on the cathode (Eq. 13 and 14), is able to react with SO_4^{2-} of the solvent, the actual compound preciptating might be $K_4(VO)_3(SO_4)_5$ that was formed by reduction of the eutectic with SO_2 (see previous section). Formation of the V(III) salt $K_3V(SO_4)_3$ could take place through the following reactions

$$VOSO_4 + SO_4^{2-} \rightleftarrows VO(SO_4)_2^{2-} \qquad [18]$$

$$VO(SO_4)_2^{2-} + e^- \rightleftarrows V(SO_4)_2^- + O^{2-} \qquad [19]$$

$$3K^+ + V(SO_4)_2^- + SO_4^{2-} \rightleftarrows K_3V(SO_4)_3 \qquad [20]$$

As V(IV), e.g., as $K_4(VO)_3(SO_4)_5$ or $VOSO_4$, is only partially soluble, and V(III), e.g., as $K_3V(SO_4)_3$ has a very low solubility,[7,35,36] peak potential shifts were due to uncompensated plating on the electrode surface. Peak heights would be expected to increase if this solidification occurred. Previously presented melting curves[1] showed a relatively conductive solid. If a conductive solid deposited on the electrode, the effective electrode area would increase, resulting in an apparent current increase. Theoretically the current density would be identical while the apparent current density increases.

Consideration of the large stripping peak I_a supports these analogies. The height and size of this oxidation peak were directly dependent on reduction levels. As more coulombs were passed at potentials greater than $E_p(I_c)$ currents were observed to rise. If species were being reduced as proposed and plating on the electrode, a stripping peak would be expected. In addition, the peak I_a potential was near the peak II_1 potential, supporting the argument that both repre-

S0013-4651(98)01-004-0 CCC: $7.00

Table IV. Attribution of peaks to possible complex reactions.

Peak	Suggested reactions
$I_c + II_c$:	$VO_3^- + SO_4^{2-} + e^- \rightleftarrows VOSO_4 + 2\ O^{2-}$
	$VO_2SO_4^- + e^- \rightleftarrows VOSO_4 + O^{2-}$
	$VO_2(SO_4)_2^{3-} + e^- \rightleftarrows VO(SO_4)_2^{2-} + O^{2-}$
Plating:	$4K^+ + 3VOSO_4 + 2SO_4^{2-} \rightarrow K_4(VO)_3(SO_4)_5$ (s)
III_c:	$VO(SO_4)_2^{2-} + e^- \rightleftarrows V(SO_4)_2^- + O^{2-}$
Plating:	$3K^+ + V(SO_4)_2^- + SO_4^{2-} \rightarrow K_3V(SO_4)_3$ (s)
I_a, Stripping:	V(III)- and V(IV)-salts → V(V)
II_1:	$VO(SO_4)_2^{2-} + O^{2-} \rightarrow VO_2(SO_4)_2^{3-} + e^-$
I_1 and II_a:	$SO_4^{2-} \rightarrow SO_3 + 1/2\ O_2 + 2e^-$

sent oxidation of vanadia; peak II_1 of V(IV) and peak I_a of V(IV) and V(III) formed at peaks I_c, II_c, and III_c.

Peak II_a is presumed to be the oxidation of available sulfate according to

$$SO_4^{2-} \rightleftarrows 2e^- + SO_3\ \frac{1}{2}O_2 \qquad [21]$$

which has been proposed by Franke and Winnick,[37] and found to exist 0.5 V from the vanadium redox couple they explored. In addition, E^0 between this sulfate oxidation and the V(V) reduction was estimated using JANAF thermochemical ΔG_f^0 data to be −2.344 at 700 K for a sulfate melts without compensation for Nernstian effects. Further, as the negative switching potential was increased, peak II_a became peak I_1, suggesting it was an identical reaction. This proof in combination with I_1 analysis and the $n = 2$ equiv/mol determined earlier left little doubt that peak IIa represented sulfate oxidation.

The change in height of peak II_a after reduction occurs is explained by the coordination ability of vanadium. As vanadium is reduced, less sulfate (or oxide) can complex per single vanadium, evidenced by the reactions presented above. This would free sulfate (or oxide) for oxidation, thereby increasing peak II_a currents, as well as shift peak potential due to concentration changes, both of which were observed. Bubbling was not readily observable due to the opaque melt and apparent viscosity. Any SO_3 produced would be effectively adsorbed by the melt.

Knowledge of the pseudo-reference was also gained through these experiments. Based on arguments presented above and potential analysis, the pseudo-reference is probably schematically represented by the reaction $V(V) + 1e^- \rightleftarrows V(IV)$ in the $SO_2/O_2/N_2$ atmosphere used at the reference electrode, due to the relative proximity of vanadia couples and sulfate oxidation peaks. Further, its potential is defined by the (reference) gas composition, which will set the V(V):V(IV) equilibrium. Even large changes in the bulk electrolyte, from which the reference electrode is isolated, will have little to no effect on the reference. The proposed reactions for the observed peaks are shown in Table IV.

It is important to note every reduction of vanadium shown results in the formation of an oxide ion, enhancing SO_3 removal. It can be concluded on the whole that the extremely large peak currents indicate high electrochemical activity of the melt, probably due to electrochemical utilization of V(V) and SO_4^{2-}. Any limit in this melt must therefore be due to mass transfer of these bulk species.

It is not possible to determine directly the concentration of the active species from estimates of diffusivities which vary widely, even if the active species had been studied. In an aluminate melt, V(V) was reported to have diffusivities of 3.7×10^{-7} cm^2/s at 1370°C and 2.1×10^{-6} cm^2/s at 1460°C.[38] V(V) was also reported to have a diffusivity of 5.9×10^{-8} cm^2/s in phosphoric acid.[39] In a LiCl/KCl melt at 450°C Scrosati and Laitinen[40] report the diffusivity of V(IV) as 2.68×10^{-5} cm^2/s. In a $K_2S_2O_7/V_2O_5$ melt, V(V) was reported to have a diffusivity of 2×10^{-6} cm^2/s at 400°C.[41] However, the concentration of K_2SO_4 and V_2O_5 can be estimated in the melt if ideal mixing and similarity between liquid and solid densities are assumed.

Table V. Diffusivities calculated from peak currents.

D (cm^2/s), $\times 10^{13}$	N_2	O_2/N_2	$SO_2/O_2/N_2$
Peak I_c	2.96	3.15	4.04
Peak I_1	0.89	0.76	1.49
Peak II_1	0.008	0.003	0.04

Total density was evaluated using

$$\frac{1}{\rho} = \sum \frac{(\text{wt }\%)_i}{\rho_i} \qquad [22]$$

as suggested by Reid et al.[42]

An effective concentration of sulfate (as K_2SO_4) was calculated as $C_{K_2SO_4} = 9.85 \times 10^{-3}$ mol/cm^3 and an effective concentration of V(V) (as V_2O_5) was calculated as $C_{V_2O_5} = 6.56 \times 10^{-3}$ mol/cm^3. Using these values of concentration, the previously obtained values of $C_i D_i^{1/2}$ shown in Table II could be used to determine diffusivity, listed in Table V. The very low diffusivities emphasize the nonidealities in the melt, suggesting strong species interaction.

Conclusions

The low-melting mixtures of V_2O_5 with K_2SO_4 allow facile reduction of the V(V) to V(IV) in oligomeric form with the concurrent release of oxide ions (O^{2-}). Further reduction to V(III) is also possible, with further oxide production. The V(III) compounds are highly insoluble in the melt, however. The oxide ions are readily neutralized by available dissolved SO_3, forming sulfate ions. Vanadium ions in the oxidation states III or IV are reoxidized to V(V) electrochemically, well positive of the potential necessary for sulfate oxidation. These results indicate that this melt will indeed be a good choice for the electrochemical membrane electrolyte: the SO_3 present in the flue gas will be readily neutralized at the cathode by oxide ions in the membrane. The V(IV) and V(III) is chemically oxidized back to V(V), and so is available again for electrochemical reduction. The relative ease of V(V) electroreduction, compared to the sulfur species, prohibits the unwanted reduction of S(VI) to lower oxidation states. At the anode, it is sulfate that is most readily electrooxidized, to SO_3 and oxygen, as desired.

Acknowledgment

The Danish National Research Council and the U.S. Department of Energy (University Coal Research Program) are thanked for financial support. Morten Jørgensen and Andreas Lundtang Paulsen, Department of Chemistry, Technical University of Denmark, are thanked for experimental assistance concerning the Raman spectroscopic investigation.

University of Petras and Institute of Chemical Engineering and High Temperature Chemical Processes assisted in meeting the publication costs of this article.

References

1. D. S. Schmidt, Ph.D. Thesis, School of Chemical Engineering, Georgia Institute of Technology, Atlanta, GA (1997).
2. D. S. Schmidt, D. M. McHenry, and J. Winnick, *J. Electrochem. Soc.*, **145**, 892 (1998).
3. D. S. Schmidt and J. Winnick, *AIChE J.*, **44**, 323 (1998).
4. S. Hähle and A. Meisel, *Kinet. Katal.*, **12**, 1276 (1971).
5. G. K. Boreskov, V. V. Illiarionov, R. P. Ozerov, and E. V. Kildisheva, *Zh. Obsch. Khim.*, **24**, 23 (1954).
6. G. Janz, *Molten Salts Handbook*, Academic Press, New York (1964).
7. O. B. Lapina, B. S. Balzhinimaev, S. Boghosian, K. M. Eriksen, and R. Fehrmann, *Catal. Today*, Submitted.
8. H. F. A. Topsoe and A. Nielsen, *Trans Dan. Acad. Tech. Sci.*, **1**, 18 (1947).
9. J. Villadsen and H. Livbjerg, *Catal. Rev.-Sci. Eng.*, **17**, 203 (1978).
10. K. Nielsen, R. Fehrmann, and K. M. Eriksen, *Inorg. Chem.*, **32**, 4825 (1993).
11. K. Nielsen, K. M. Eriksen, and R. Fehrmann, In preparation.
12. D. A. Karydis, K. M. Eriksen, R. Fehrmann, and S. Boghosian, *J. Chem. Soc., Dalton Trans.*, 2151 (1994).

S0013-4651(98)01-004-0 CCC: $7.00

13. K. M. Eriksen, D. A. Karydis, S. Boghosian, and R. Fehrmann, *J. Catal.*, **155**, 32 (1995).
14. S. Boghosian and G. N. Papatheodorou, *J. Phys. Chem.*, **93**, 415 (1989).
15. G. K. Boreskov, V. A. Dzisko, D. V. Tarasova, and G. P. Balaganskaya, *Kinet. I Katal.*, **11**, 144 (1970).
16. *JANAF Thermochemical Tables*, 3rd ed., M. W. Chase, Jr. et al. Editors, U.S. Secretary of Commerce, Washington, DC (1986).
17. S. Boghosian, F. Borup, and A. Chrissanthopoulos, *Catal. Lett.*, **48**, 145 (1997).
18. A. Chrissanthopoulos, F. Borup, R. Fehrmann, and S. Boghosian, To be submitted.
19. Z. X. Shen, C. W. Ong, S. H. Tang, and M. H. Kuok, *Phys. Rev. B*, **49**. 1433 (1994).
20. S. Boghosian, R. Fehrmann, and K. Nielsen, *Acta. Chem. Scand.*, **48**, 724 (1994).
21. R. Fehrmann, S. Boghosian, G. N. Papatheodorou, K. Nielsen, R. Berg, and N. J. Bjerrum, *Inorg. Chem.*, **28**, 1847 (1989).
22. Y. Isreal and L. Meites, *Encyclopedia of Electrochemistry of the Elements*, Vol. VII, A. J. Bard, Editor, Chap. "VII-2 Vanadium," Marcel Dekker, Inc., New York (1976).
23. I. N. Belyaev, T. G. Lupeiko, and V. P. Braitsev, *Russ. J. Inorg. Chem.*, **18**, 1331 (1973).
24. R. Fehrmann, M. Gaune-Escard, and N. J. Bjerrum, *Inorg. Chem.*, **25**, 1132 (1986).
25. O. B. Lapina, V. M. Mastikhin, A. A. Shubin, K. M. Eriksen, and R. Fehrmann, *J. Mol. Catal*., **99**, 123 (1995).
26. O. B. Lapina, V. Terskikh, A. A. Shubin, V. M. Mastikhin, K. M. Eriksen, and R. Fehrmann, *J. Phys. Chem.*, **101**, 9188 (1997).
27. F. D. Hardcastle and I. E. Wachs, *J. Phys. Chem.*, **95**, 5031 (1991).
28. M. D. Franke and J. Winnick, *J. Electroanal. Chem.*, **238**, 163 (1987).
29. Z. G. Bazarova, G. K. Boreskov, A. A. Ivanov, L. G. Karakchiev, and L. D. Kockina, *Kinet. Catal*., **7**, 399 (1971).
30. A. Durand, G. Picard, and J. Vedel, *J. Electroanal. Chem.*, **127**, 169 (1981).
31. N. J. Bjerrum, I. M. Petrushina, and R. W. Berg, *J. Electrochem. Soc.*, **142**, 1806 (1995).
32. M. Dojcinovic, M. Susic, and S. Mentus, *J. Mol. Cat.*, **11**, 275 (1981).
33. C. R. Wolfe and R. D. Caton, *Anal. Chem.*, **43**, 663 (1971).
34. H. A. Laitinen and D. H. Rhodes, *J. Electrochem. Soc*.,**109**, 413 (1962).
35. S. G. Masters, A. Chrissanthopoulos, K. M. Eriksen, S. Boghosian, and R. Fehrmann, *J. Catal.*, **166**, 16 (1997).
36. S. Boghosian, R. Fehrmann, N. J. Bjerrum, and G. N. Papatheodorou, *J. Catal.*, **119**, 121 (1989).
37. M. D. Franke and J. Winnick, *J. Appl. Electrochem.*, **19**, 10 (1988).
38. V. N. Boronenkov, O. A. Esin, and P. M. Shurigin, *Russ. J. Phys. Chem*., **38**, 628 (1964).
39. I. M. Kolthoff and E. R. Nightingale, *Anal. Chim. Acta*, **17**, 32 (1957).
40. B. Scrosati and H. A. Laitinen, *Anal. Chem*., **36**, 15 (1964).
41. M. D. Franke, Ph.D. Thesis, School of Chemical Engineering, Georgia Instistute of Technology, Atlanta, Georgia (1988).
42. R. C. Reid, J. M. Prausnitz, and B. E. Poling, *The Properties of Gases and Liquids*, 4th ed., p. 89, McGraw-Hill, New York (1987).